

**Cover page**

Title: Decentralized  $\mathcal{H}_\infty$  Controller Design for Large-scale Wireless Structural Sensing and Control Systems

Authors: Yang Wang  
Jerome P. Lynch  
Kincho H. Law

## ABSTRACT

Wireless structural sensing has attracted much research interest in recent years. With actuation functionality incorporated in the design of the wireless sensing nodes, a wireless feedback structural control system can be constructed. For wireless structural control systems that face challenges in communication range, latency, and reliability, decentralized system architectures can provide promising solutions. This paper examines the use of a decentralized controller that minimizes the  $\mathcal{H}_\infty$  norm of a closed-loop system. Decentralized control solutions are developed for both continuous-time and discrete-time formulations. To evaluate the performance of the decentralized  $\mathcal{H}_\infty$  controller design, numerical simulations of the wireless control system are conducted using a 20-story benchmark structure with different decentralized system architectures.

## INTRODUCTION

Real-time feedback control has been a topic of great interest to the structural engineering community in the last few decades [1]. A feedback structural control system includes a network of sensors, controllers, and actuators. In traditional feedback control systems, large amount of coaxial wiring is needed to connect the sensors, controllers, and actuators into an integrated system that features a feedback control loop. The cost for installing wires grows significantly as the size of the structure and the number of sensors and control devices increase. Furthermore, once a wired control system is installed in a structure, it could be quite costly to change the system architecture and to reroute the wires. To eliminate the cost and inconvenience of tethered installations, wireless communication and embedded computing technologies can be a viable alternative in structural control systems. In a prototype wireless control system [2], wireless communication replaces wired communication for the exchange of data between sensors and controllers. The distributed network of

wireless sensors can be collocated with individual structural actuators for the calculation and execution of control forces.

In a centralized control system, regardless of the communication medium (wireless or wired), the central controller has to collect data from all the sensors in the structure. Requirements on communication range and data transmission rate increase with the size of the structure and the number of sensors being deployed. For a wireless control system, these communication issues could potentially present difficulty for large-scale implementations. Furthermore, the centralized control server represents a point of potential bottleneck failure for the whole system. Decentralized control strategies could be deployed to overcome some of the inherent problems of a centralized control system [3, 4]. In decentralized control systems, multiple controllers are distributed throughout the structure. Requiring data only from neighboring sensors, each controller commands actuators in its vicinity. As a result, shorter communication range and lower data transmission rate are required.

To ensure a suitable level of performance of the decentralized wireless control system, decentralized controller design based on the linear quadratic regulator (LQR) optimization criteria has been studied [4]. This paper explores a different control methodology, namely the  $\mathcal{H}_\infty$  control theory that can offer excellent control performance when “worst-case” external disturbances are encountered.  $\mathcal{H}_\infty$  controller design is also convenient when model uncertainties exist (as is typical in most civil structures). Centralized  $\mathcal{H}_\infty$  design in the continuous-time domain for civil structural control has been studied by many researchers [5, 6]. One important feature of  $\mathcal{H}_\infty$  control is that the controller design can be formulated using linear matrix inequalities (LMI) [8]. For an optimization problem with LMI constraints, sparsity patterns can be easily applied to the matrix variables. This property can be utilized to design decentralized controllers where the gain matrices with certain sparsity patterns represent decentralized information feedback. This paper explores the feasibility of designing decentralized  $\mathcal{H}_\infty$  controllers that may be potentially employed in decentralized wireless structural control systems. Decentralized  $\mathcal{H}_\infty$  controller design in both the continuous-time and discrete-time domains are investigated. Numerical simulations using a 20-story benchmark structure are conducted to illustrate the efficacy of the decentralized  $\mathcal{H}_\infty$  controller design employed in different wireless structural control architectures.

## CONTINUOUS-TIME DECENTRALIZED $\mathcal{H}_\infty$ CONTROL

For a lumped-mass structural model with  $n$  degrees-of-freedom (DOF) and  $m$  actuators, the state-space representation can be formulated as [1]:

$$\dot{\mathbf{x}}_I(t) = \mathbf{A}_I \mathbf{x}_I(t) + \mathbf{B}_I \mathbf{u}(t) + \mathbf{E}_I \mathbf{w}(t) \quad (1)$$

where  $\mathbf{x}_I = [\mathbf{q}(t); \dot{\mathbf{q}}(t)]$  is the state vector;  $\mathbf{q}(t)$  is the  $n \times 1$  displacement vector relative to the ground;  $\mathbf{u}(t)$  and  $\mathbf{w}(t)$  are the  $m \times 1$  control force and  $r \times 1$  external excitation vectors, respectively;  $\mathbf{A}_I$ ,  $\mathbf{B}_I$ , and  $\mathbf{E}_I$  are the  $2n \times 2n$  system,  $2n \times m$  actuator

location, and  $2n \times r$  excitation location matrices, respectively. In this study, it is assumed that inter-story drifts and velocities are observable. The displacement and velocity variables in  $\mathbf{x}_I$ , which are relative to the ground, are first transformed into drifts and velocities between neighboring floors. That is, the inter-story drift and velocity at each floor are grouped together as  $\mathbf{x} = [q_1; \dot{q}_1; q_2 - q_1; \dot{q}_2 - \dot{q}_1; \dots; q_n - q_{n-1}; \dot{q}_n - \dot{q}_{n-1}]$ . A linear transformation matrix  $\mathbf{\Gamma}$  can be defined such that  $\mathbf{x} = \mathbf{\Gamma}\mathbf{x}_I$ . Substituting  $\mathbf{x}_I = \mathbf{\Gamma}^{-1}\mathbf{x}$  into Eq. (1) and left-multiplying the equation with  $\mathbf{\Gamma}$ , the state space representation with the transformed state vector becomes:

$$\dot{\mathbf{x}}(t) = \mathbf{A}\mathbf{x}(t) + \mathbf{B}\mathbf{u}(t) + \mathbf{E}\mathbf{w}(t) \quad (2)$$

where  $\mathbf{A} = \mathbf{\Gamma}\mathbf{A}_I\mathbf{\Gamma}^{-1}$ ,  $\mathbf{B} = \mathbf{\Gamma}\mathbf{B}_I$ ,  $\mathbf{E} = \mathbf{\Gamma}\mathbf{E}_I$ . The system output  $\mathbf{z}(t)$  is defined as the sum of linear transformations to the state vector  $\mathbf{x}(t)$  and the control vector  $\mathbf{u}(t)$ :

$$\mathbf{z}(t) = \mathbf{C}_z\mathbf{x}(t) + \mathbf{D}_z\mathbf{u}(t) \quad (3)$$

where  $\mathbf{C}_z$  and  $\mathbf{D}_z$  are the output matrices for the state and control force vectors, respectively. Assuming static state feedback, the control force  $\mathbf{u}(t)$  is decided by  $\mathbf{u}(t) = \mathbf{G}\mathbf{x}(t)$ , where  $\mathbf{G}$  is termed the control gain matrix. Substituting  $\mathbf{G}\mathbf{x}(t)$  for  $\mathbf{u}(t)$  in Eq. (2) and Eq. (3), the state-space equations of the closed-loop system can be written as:

$$\dot{\mathbf{x}}(t) = \mathbf{A}_{CL}\mathbf{x}(t) + \mathbf{E}\mathbf{w}(t), \text{ and } \mathbf{z}(t) = \mathbf{C}_{CL}\mathbf{x}(t) \quad (4)$$

where  $\mathbf{A}_{CL} = \mathbf{A} + \mathbf{B}\mathbf{G}$ , and  $\mathbf{C}_{CL} = \mathbf{C}_z + \mathbf{D}_z\mathbf{G}$ . In the frequency-domain, the system dynamics can be represented by the transfer function  $\mathbf{H}_{zw}(s)$  from disturbance  $\mathbf{w}(t)$  to output  $\mathbf{z}(t)$  as [7]:

$$\mathbf{H}_{zw}(s) = \mathbf{C}_{CL}(s\mathbf{I} - \mathbf{A}_{CL})^{-1}\mathbf{E} \quad (5)$$

where  $s$  is the complex Laplacian variable. The objective of  $\mathcal{H}_\infty$  control is to minimize the  $\mathcal{H}_\infty$ -norm of the transfer function with  $s$  on the imaginary axis:

$$\|\mathbf{H}_{zw}\|_\infty = \sup_{\omega} \bar{\sigma}[\mathbf{H}_{zw}(j\omega)] = \sup_{\mathbf{w}, \|\mathbf{w}(t)\|_2 \neq 0} \left( \frac{\|\mathbf{z}(t)\|_2}{\|\mathbf{w}(t)\|_2} \right) \quad (6)$$

where  $\omega$  represents the frequency,  $\bar{\sigma}[\cdot]$  denotes the maximum singular value of a matrix, and ‘‘sup’’ denotes the supremum of a set of real numbers. By minimizing the peak of the maximum singular value of the transfer function over the entire frequency span, the system output can be greatly reduced when worst-case disturbances are applied to the system. Note that the  $\|\mathbf{H}_{zw}\|_\infty$  norm has an equivalent interpretation in the time domain, as the supremum of the 2-norm amplification from the disturbance to the output, where the 2-norm of a signal  $\mathbf{f}(t)$  is defined as  $\|\mathbf{f}(t)\|_2 = \sqrt{\int_{-\infty}^{\infty} \mathbf{f}^T(t)\mathbf{f}(t)dt}$ . Following the Bounded Real Lemma, the following two statements are equivalent for a  $\gamma$ -suboptimal  $\mathcal{H}_\infty$  controller design [8]:

- (i)  $\|\mathbf{H}_{zw}\|_\infty < \gamma$ , and  $\mathbf{A}_{CL}$  is stable in continuous-time sense (i.e. the real parts of all the eigenvalues of  $\mathbf{A}_{CL}$  are negative);
- (ii) There exists a symmetric matrix  $\mathbf{\Theta} > 0$  s.t. following inequalities hold:

$$\begin{bmatrix} \mathbf{A}_{CL}\mathbf{\Theta} + \mathbf{\Theta}\mathbf{A}_{CL}^T + \mathbf{E}\mathbf{E}^T/\gamma^2 & \mathbf{\Theta}\mathbf{C}_{CL}^T \\ * & -\mathbf{I} \end{bmatrix} < 0 \quad (7)$$

where \* denotes the symmetric entry. Using the closed-loop matrix definitions in Eq. (4), Eq. (7) becomes:

$$\begin{bmatrix} \mathbf{A}\mathbf{\Theta} + \mathbf{\Theta}\mathbf{A}^T + \mathbf{B}\mathbf{G}\mathbf{\Theta} + \mathbf{\Theta}\mathbf{G}^T\mathbf{B}^T + \mathbf{E}\mathbf{E}^T/\gamma^2 & \mathbf{\Theta}\mathbf{C}_z^T + \mathbf{\Theta}\mathbf{G}^T\mathbf{D}_z^T \\ * & -\mathbf{I} \end{bmatrix} < 0 \quad (8)$$

The above nonlinear matrix inequalities can be converted into a set of linear matrix inequalities (LMI) by introducing a new variable  $\mathbf{Y} = \mathbf{G}\mathbf{\Theta}$ :

$$\begin{bmatrix} \mathbf{A}\mathbf{\Theta} + \mathbf{\Theta}\mathbf{A}^T + \mathbf{B}\mathbf{Y} + \mathbf{Y}^T\mathbf{B}^T + \mathbf{E}\mathbf{E}^T/\gamma^2 & \mathbf{\Theta}\mathbf{C}_z^T + \mathbf{Y}^T\mathbf{D}_z^T \\ * & -\mathbf{I} \end{bmatrix} < 0 \quad (9)$$

In summary, the continuous-time  $\gamma$ -suboptimal  $\mathcal{H}_\infty$  control problem is now transformed into a convex optimization problem: the decision variables are  $\mathbf{Y}$ ,  $\mathbf{\Theta}$ , and  $\gamma$ ; the objective is to minimize  $\gamma$ ; and the constraints are  $\mathbf{\Theta} > 0$  and the LMI expressed in Eq. (9). Numerical solutions to this optimization problem can be computed, for example, using the Matlab LMI Toolbox [9]. After the optimization problem is solved, the  $\gamma$ -suboptimal control gain matrix is computed as:

$$\mathbf{G} = \mathbf{Y}\mathbf{\Theta}^{-1} \quad (10)$$

In general, the algorithm finds a gain matrix without any sparsity constraints, which represents a control scheme with centralized state feedback. Gain matrices for decentralized state feedback control can be found by applying appropriate sparsity constraints to the optimization variables  $\mathbf{Y}$  and  $\mathbf{\Theta}$ .

## DISCRETE-TIME DECENTRALIZED $\mathcal{H}_\infty$ CONTROL

For implementation in the microcontrollers of the wireless sensing and control units, a discrete-time decentralized  $\mathcal{H}_\infty$  controller design is developed. The continuous-time system in Eq. (4) can be equivalently formulated as a discrete-time system [1]:

$$\mathbf{x}_d[k+1] = \mathbf{A}_{dCL}\mathbf{x}_d[k] + \mathbf{E}_d\mathbf{w}_d[k], \text{ and } \mathbf{z}_d[k] = \mathbf{C}_{dCL}\mathbf{x}_d[k] \quad (11)$$

where the subscript “d” indicates that the variables are expressed in discrete-time domain, and the closed-loop system matrices  $\mathbf{A}_{dCL}$  and  $\mathbf{C}_{dCL}$  are defined accordingly. For linear state feedback, the control force  $\mathbf{u}_d[k]$  is decided as  $\mathbf{u}_d[k] = \mathbf{G}_d\mathbf{x}_d[k]$ . Following the Bounded Real Lemma, the following two statements are equivalent for discrete-time systems [7]:

- (i) The  $\mathcal{H}_\infty$ -norm of the closed-loop system in Eq.(11) is less than  $\gamma$ , and  $\mathbf{A}_{dCL}$  is stable in the discrete-time sense (i.e. all of the eigenvalues of  $\mathbf{A}_{dCL}$  fall in the unit circle on the complex plane);
- (ii) There exists a symmetric matrix  $\bar{\Theta}_d > 0$  s.t. the following inequalities hold:

$$\begin{bmatrix} \mathbf{A}_{dCL}^T & \mathbf{C}_{dCL}^T/\gamma \\ \mathbf{E}_d^T & \mathbf{0} \end{bmatrix} \begin{bmatrix} \bar{\Theta}_d & \mathbf{0} \\ \mathbf{0} & \mathbf{I} \end{bmatrix} \begin{bmatrix} \mathbf{A}_{dCL} & \mathbf{E}_d \\ \mathbf{C}_{dCL}/\gamma & \mathbf{0} \end{bmatrix} - \begin{bmatrix} \bar{\Theta}_d & \mathbf{0} \\ \mathbf{0} & \mathbf{I} \end{bmatrix} < 0 \quad (12)$$

Replacing  $\bar{\Theta}_d$  with  $\tilde{\Theta}_d/\gamma^2$  and using Schur complements [8], the above matrix inequalities can be shown as equivalent to:

$$\begin{bmatrix} \tilde{\Theta}_d & \mathbf{0} & \mathbf{A}_{dCL}^T \tilde{\Theta}_d & \mathbf{C}_{dCL}^T \\ * & \gamma^2 \mathbf{I} & \mathbf{E}_d^T \tilde{\Theta}_d & \mathbf{0} \\ * & * & \tilde{\Theta}_d & \mathbf{0} \\ * & * & * & \mathbf{I} \end{bmatrix} > 0 \quad (13)$$

Left-multiplying and right-multiplying the above matrix with a positive definite matrix  $\text{diag}(\tilde{\Theta}_d^{-1}, \mathbf{I}, \tilde{\Theta}_d^{-1}, \mathbf{I})$ , and letting  $\Theta_d = \tilde{\Theta}_d^{-1}$ , the following matrix inequalities are obtained:

$$\begin{bmatrix} \Theta_d & \mathbf{0} & \Theta_d \mathbf{A}_{dCL}^T & \Theta_d \mathbf{C}_{dCL}^T \\ * & \gamma^2 \mathbf{I} & \mathbf{E}_d^T & \mathbf{0} \\ * & * & \Theta_d & \mathbf{0} \\ * & * & * & \mathbf{I} \end{bmatrix} > 0 \quad (14)$$

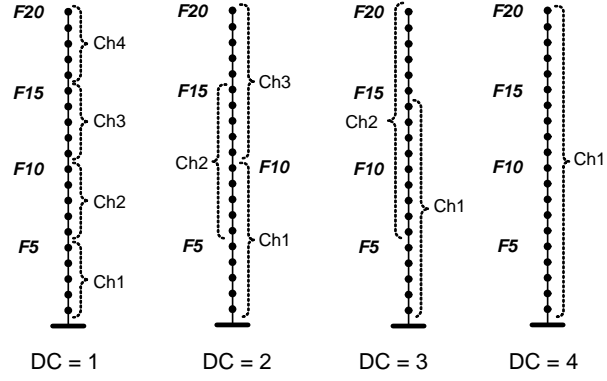
Similar to the continuous-time system, by replacing the closed-loop matrices  $\mathbf{A}_{dCL}$  and  $\mathbf{C}_{dCL}$  in Eq. (14), and letting  $\mathbf{Y}_d = \mathbf{G}_d \Theta_d$ , the discrete-time  $\gamma$ -suboptimal  $\mathcal{H}_\infty$  control problem can be converted to a convex optimization problem with LMI constraints. Furthermore, sparsity patterns of the gain matrix can be achieved by applying appropriate sparsity patterns to the LMI variables  $\mathbf{Y}_d$  and  $\Theta_d$ .

## NUMERICAL EXAMPLE

Since the discrete-time formulation is particularly suitable for implementation in digital controllers, such as the wireless sensing and actuation units developed [4], numerical simulation results are presented using the discrete-time  $\mathcal{H}_\infty$  controllers. A 20-story benchmark structure designed for the SAC project is selected [10]. To simplify the analysis, the building is modeled as an in-plane lumped-mass structure with one actuator allocated between each two neighboring floors. Fig. 1(a) shows the mass, stiffness, and damping parameters of the structure. In the numerical simulations, it is assumed that both the inter-story drifts and inter-story velocities between every two neighboring floors are observable. As shown in Eq. (2), the state-space equations are formulated such that the state-space vector contains inter-story drifts and velocities. For the simulations presented here, matrices  $\mathbf{C}_z$  and  $\mathbf{D}_z$  are defined as:

Seismic Mass	
F1	$1.126 \times 10^6$ kg
F2 – F19	$1.100 \times 10^6$ kg
F20	$1.170 \times 10^6$ kg
Inter-story Stiffness	
F1-F5	$862.07 \times 10^3$ kN/m
F6-F11	$554.17 \times 10^3$ kN/m
F12-F14	$453.51 \times 10^3$ kN/m
F15-F17	$291.23 \times 10^3$ kN/m
F18-F19	$256.46 \times 10^3$ kN/m
F20	$171.70 \times 10^3$ kN/m
Damping	
5% Natural Damping	

(a)



(b)

Figure 1. Twenty-story SAC building for numerical simulations: (a) model parameters of the lumped mass structure; (b) wireless subnet partitioning for different degrees of centralization (DC).

$$\mathbf{C}_z = \begin{bmatrix} 10^7 \mathbf{C}_{z1} \\ \mathbf{0}_{20 \times 40} \end{bmatrix}, \quad \mathbf{D}_z = \begin{bmatrix} \mathbf{0}_{40 \times 20} \\ 10^{-7} \mathbf{I}_{20 \times 20} \end{bmatrix} \quad (15)$$

where  $\mathbf{C}_{z1}$  is a  $40 \times 40$  diagonal matrix, whose diagonal entries are  $\sqrt{20}, \sqrt{20}, \sqrt{19}, \sqrt{19}, \dots, \sqrt{2}, \sqrt{2}, 1, 1$ . Simulations are conducted for different decentralization schemes as shown in Fig. 1(b). The degrees of centralization (DC) reflect the different wireless network architectures, with each wireless channel representing one subnet of the global system. The actuators covered by a subnet are allowed to access the wireless sensor data within that subnet. For example, the case where  $DC = 1$  implies each wireless channel covers only five stories and a total of four wireless channels (subnets) are utilized; the case where  $DC = 2$  implies each wireless channel covers ten stories and a total of three wireless channels are utilized. The gain matrices for these two decentralized information structures have the following sparsity patterns:

$$\mathbf{G}_d = \begin{bmatrix} \blacksquare & & & & \\ & \blacksquare & & & \\ & & \blacksquare & & \\ & & & \blacksquare & \\ & & & & \blacksquare \end{bmatrix}_{20 \times 40} \quad \text{when } DC = 1; \quad \mathbf{G}_d = \begin{bmatrix} \blacksquare & \blacksquare & & & \\ \blacksquare & \blacksquare & \blacksquare & & \\ & \blacksquare & \blacksquare & \blacksquare & \\ & & \blacksquare & \blacksquare & \blacksquare \\ & & & \blacksquare & \blacksquare \end{bmatrix}_{20 \times 40} \quad \text{when } DC = 2 \quad (16)$$

Each entry in the above matrices represents a  $5 \times 10$  block submatrix. To achieve the sparsity patterns, the matrix  $\mathbf{Y}_d$  is defined to have the same sparsity pattern as  $\mathbf{G}_d$ , and  $\mathbf{\Theta}_d$  is defined to be block-diagonal. For the cases where  $DC = 3$  and  $DC = 4$ , the number of stories covered by each wireless subnet increases accordingly.

To investigate the effectiveness of the proposed decentralized controller design, we assume the 20-story structure is instrumented with ideal actuators that produce any desired horizontal force between every two neighboring floors. Simulations are performed for different centralization degrees ( $DC = 1, \dots, 4$ ) and sampling periods (ranging from 0.01s to 0.06s at a resolution of 0.01s). Additionally, three ground motion records all scaled to a peak ground acceleration (PGA) of  $1\text{m/s}^2$  are used for the simulation: the 1940 El Centro NS record (Imperial Valley Irrigation District Station), the 1995 Kobe NS record (JMA Station), and the 1999 Chi-Chi NS record (TCU-076 Station). Two representative performance indexes are adopted:

$$PI_1 = \max_{\text{Earthquakes}} \left\{ \max_{k,i} d_i[k] / \max_{k,i} \hat{d}_i[k] \right\}, \text{ and } PI_2 = \max_{\text{Earthquakes}} \left\{ \|\mathbf{z}_d\|_2 / \|\hat{\mathbf{z}}_d\|_2 \right\} \quad (17)$$

Here  $PI_1$  and  $PI_2$  are the performance indexes corresponding to inter-story drifts and the output vector  $\mathbf{z}_d$ , respectively. In Eq. (17),  $d_i[k]$  represents the inter-story drift between floor  $i$  ( $i = 1, \dots, n$ ) and its lower floor at time step  $k$ , and  $\max_{k,i} d_i[k]$  is the maximum inter-story drift over the entire time history and among all floors. The maximum inter-story drift is normalized by its counterpart  $\max_{k,i} \hat{d}_i[k]$ , which is the maximum response of the uncontrolled structure. The largest normalized ratio among the simulations for the three different earthquake records is defined as the performance index  $PI_1$ . Similarly, the performance index  $PI_2$  is defined based on the 2-norm of the output vector  $\mathbf{z}_d$ , i.e.  $\|\mathbf{z}_d\|_2 = \sum_{k=1}^K \mathbf{z}_d^T[k] \mathbf{z}_d[k]$ , where  $K$  denotes the last time step for the duration of the simulation. When computing the two indexes, a uniform time step of 0.001s is used to collect the structural response data points for  $d_i[k]$  and  $\mathbf{z}_d[k]$ , regardless of the sampling period of the control scheme.

Fig. 2 shows the control performance indexes for different degrees of centralization and sampling periods. Generally speaking, control performance is better for higher degrees of centralization and shorter sampling periods. The plots show that except for the case where  $DC = 1$ , other control schemes with information overlapping achieve comparable performance. To better review the simulation results,

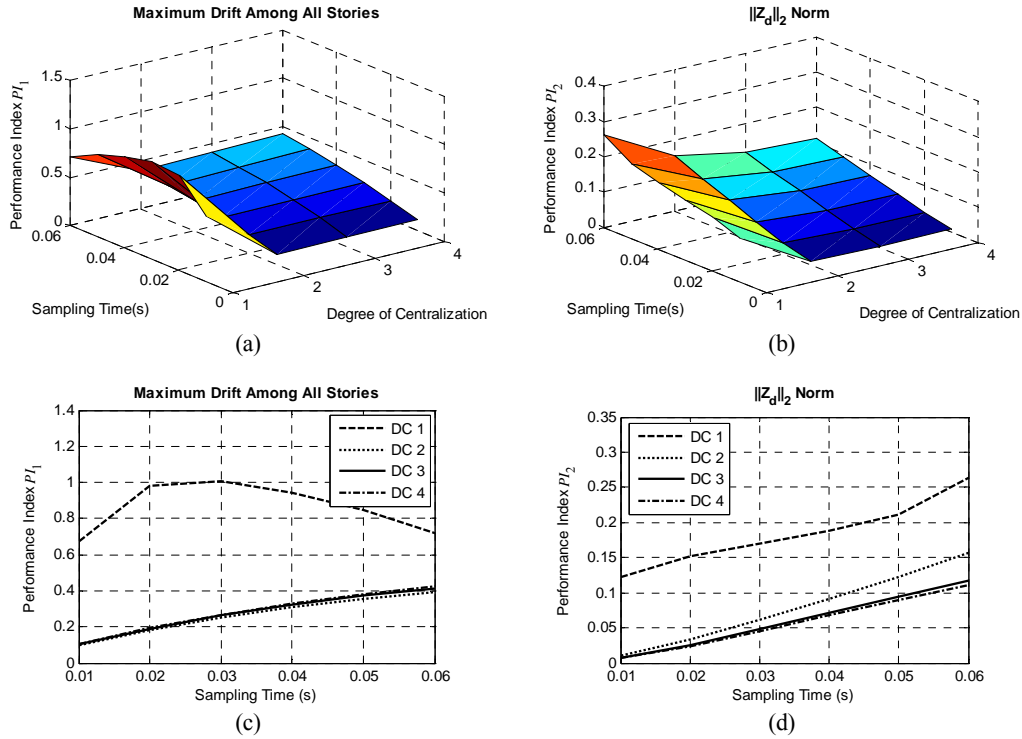


Figure 2. Simulation results for the 20-story SAC Building instrumented with ideal actuators. The plots illustrate performance indexes for different sampling time steps and degrees of centralization (DC): (a) 3D plot for performance index  $PI_1$ ; (b) 3D plot for performance index  $PI_2$ ; (c) condensed 2D plot for  $PI_1$ ; (d) condensed 2D plot for  $PI_2$ .

the performance indexes for the four different control schemes are re-plotted as a function of sampling period in Fig. 2(c) and 2(d). It is observed that if shorter sampling periods are achieved in partially decentralized control systems, the system performance can be better than centralized systems with longer sampling periods.

## SUMMARY AND CONCLUSION

This paper discusses decentralized structural control design that minimizes the system  $\mathcal{H}_\infty$  norm with potential applications to wireless structural sensing and control systems. Solutions are developed for both continuous-time and discrete-time formulations. Numerical simulation results using a 20-story benchmark structure illustrate the performance of the decentralized controller design. Future research in decentralized  $\mathcal{H}_\infty$  controller design may utilize system measurement feedback and consider time delay effects in the design. Comparative study will be conducted between the decentralized  $\mathcal{H}_\infty$  controller design and the previously proposed decentralized controller design based on LQR criteria [4].

## ACKNOWLEDGEMENT

This research is partially funded by the National Science Foundation under grant CMS-0528867 and the Office of Naval Research Young Investigator Program awarded to Prof. Jerome P. Lynch at the University of Michigan. The first author was supported by the Office of Technology Licensing Stanford Graduate Fellowship.

## REFERENCES

1. Soong, T.T. 1990. *Active Structural Control: Theory and Practice*. Wiley, Harlow, Essex, England.
2. Wang, Y., R.A. Swartz, J.P. Lynch, K.H. Law, K.-C. Lu, and C.-H. Loh. 2006. "Wireless feedback structural control with embedded computing," *Proceedings of the SPIE 11th International Symposium on Nondestructive Evaluation for Health Monitoring and Diagnostics*, February 26 - March 2, 2006.
3. Sandell, N., Jr., P. Varaiya, M. Athans, and M. Safonov. 1978. "Survey of decentralized control methods for large scale systems," *IEEE T. Automat. Contr.*, **23**(2):108-128.
4. Wang, Y., R.A. Swartz, J.P. Lynch, K.H. Law, K.-C. Lu, and C.-H. Loh. 2007. "Decentralized civil structural control using real-time wireless sensing and embedded computing," *Smart Struct. Syst.*:in press.
5. Yang, J.N., S. Lin, and F. Jabbari. 2004. " $H_\infty$ -based control strategies for civil engineering structures," *Struct. Control Hlth.*, **11**(3):223-237.
6. Balandin, D.V. and M.M. Kogan. 2005. "LMI-based optimal attenuation of multi-storey building oscillations under seismic excitations," *Struct. Control Hlth.*, **12**(2):213-224.
7. Zhou, K., J.C. Doyle, and K. Glover. 1996. *Robust and Optimal Control*. Prentice Hall, Englewood Cliffs, NJ.
8. Boyd, S.P., L. El Ghaoui, E. Feron, and V. Balakrishnan. 1994. *Linear Matrix Inequalities in System and Control Theory*. SIAM, Philadelphia, PA.
9. Gahinet, P. 1995. *LMI Control Toolbox for Use with MATLAB*. MathWorks Inc., Natick, MA.
10. Spencer, B.F., Jr., R.E. Christenson, and S.J. Dyke. 1998. "Next generation benchmark control problem for seismically excited buildings," *Proceedings of the 2nd World Conference on Structural Control*, June 29 -July 2, 1998.